Middle Miocene reworked turbidites in the Baiyun Sag of the Pearl River Mouth Basin, northern South China Sea margin: Flow…

Article *in* Journal of Asian Earth Sciences · June 2016

DOI: 10.1016/j.jseaes.2016.06.025

Chenglin Gong
University of Texas at Austin

Yingmin Wang
China University of Petroleum

F. Javier Hernández-Molina
Royal Holloway, University of London

D. A. V. Stow
Heriot-Watt University

Journal of Asian Earth Sciences xxx (2016) xxx–xxx

Contents lists available at ScienceDirect

Journal of Asian Earth Sciences

journal homepage: www.elsevier.com/locate/jseaes

Full length Article

Middle Miocene reworked turbidites in the Baiyun Sag of the Pearl River Mouth Basin, northern South China Sea margin: Processes, genesis, and implications

Chenglin Gong [a,*], Yingmin Wang [b], Rongcai Zheng [c], F. Javier Hernández-Molina [d], Yun Li [c], Dorrik Stow [e], Qiang Xu [f], Rachel E. Brackenridge [e]

[a] *Department of Geological Sciences, Jackson School of Geosciences, University of Texas, Austin, TX 78712, USA*
[b] *State Key Laboratory of Petroleum Resources and Prospecting (China University of Petroleum, Beijing), Beijing, China*
[c] *State Key Laboratory of Oil & Gas Reservoirs and Exploration, Chengdu, Sichuan Province 610059, China*
[d] *Department of Earth Sciences, Royal Holloway University of London, Egham, Surrey TW20 0EX, UK*
[e] *Institute of Petroleum Engineering, Heriot Watt University, Edinburgh EH14 4AS, UK*
[f] *CNOOC Research Center, Beijing 100027, China*

ARTICLE INFO

Article history:
Received 5 January 2016
Received in revised form 18 May 2016
Accepted 24 June 2016
Available online xxxx

Keywords:
Reworked turbidites
Bottom currents
Turbidity flows
Internal waves and tides
Northern South China Sea margin

ABSTRACT

Our understanding of reworked turbidites is still in its infancy, and their flow processes and genesis still remain understudied. Core data from the middle Miocene Zhujiang Formation in the Pearl River Mouth Basin allow us to differentiate reworked turbidites, yielding two main contributions. Firstly, reworked turbidites are distinguished from turbidites by the association of traction structures and tidal signatures, which occur in discrete units rather than forming a classic "Bouma Sequence" for turbidites. Sedimentological characteristics of reworked turbidites proposed here will help to obtain a robust set of diagnostic criteria for the recognition of deep-water non-turbidite deepwater units as reservoirs. Secondly, our results suggest that, in the down-slope direction, classic detritus carried in turbidity flows would synchronously be bidirectionally reworked by internal tides and waves, resulting in tidal signatures seen in the interpreted reworked turbidites. In the along-slope direction, upper parts of dilute turbidity currents would mix vertically with seawater, and muddy fines would be winnowed away by contour currents, whereas lower parts of dilute turbidity currents would probably drop their coarse particles, resulting in traction structures recognized in the documented reworked turbidites. Our work highlights the influence of bottom currents on the development and modification of turbidites and suggests that reworked turbidites were created by the combined action of down-slope transport and reworking and along-slope winnowing and sorting, helping to better understand flow processes and genesis of non-turbidite reservoirs with a great economic interest.

Published by Elsevier Ltd.

1. Introduction

It is now widely accepted that deepwater is not only the realm of turbidity currents and that bottom currents (i.e., any 'persistent' ocean currents near the seafloor) are equally significant in transporting and depositing sediments in deep-marine environments (e.g., Hernández-Molina et al., 2006, 2011, 2014; Shanmugam, 2008a, 2012; Mutti and Carminatti, 2012; Stow et al., 2013). In addition to sandy mass-transport deposits and turbidites, sandy contourites and reworked turbidites constitute important petroleum reservoirs and are an important part of the spectrum of deep-water deposits (Shanmugam, 2008a, 2012, 2013; Stow et al., 2011, 2013; Gong et al., 2013). Sandy contourites, reworked turbidites or bottom current-reworked sands have been recognized in the Gulf of Cadiz (e.g., Nelson et al., 1993, 1999; Hernández-Molina et al., 2006, 2011, 2014; Stow et al., 2011, 2013; Brackenridge et al., 2013), the Brazilian marginal basins (Viana, 2008; Mutti and Carminatti, 2012), the Gulf of Mexico (Shanmugam et al., 1993), the Mozambique Basin (Palermo et al., 2014), and on the northern South China Sea margin (e.g., Zhu et al., 2010; Li et al., 2012; He et al., 2013; Gong et al., 2013, 2015). More than 80% of 2 million barrels of oil (boe) daily production in the Brazilian marginal basins come from the Cretaceous and Tertiary deep-water sandstones, a large proportion of which has been interpreted as reworked turbidite or sandy contourites by

---

* Corresponding author.
E-mail address: chenglingong@hotmail.com (C. Gong).

http://dx.doi.org/10.1016/j.jseaes.2016.06.025
1367-9120/Published by Elsevier Ltd.

Please cite this article in press as: Gong, C., et al. Middle Miocene reworked turbidites in the Baiyun Sag of the Pearl River Mouth Basin, northern South China Sea margin: Processes, genesis, and implications. Journal of Asian Earth Sciences (2016), http://dx.doi.org/10.1016/j.jseaes.2016.06.025

Mutti and Carminatti (2012). Sandy contourites and reworked turbidites, therefore, represent an extremely significant group of deep-water reservoirs. Understanding of sandy contourites or reworked turbidites, however, is still very much in its infancy and has only recently been pushed forward, due hydrocarbon exploration activities progressively move into greater water depths (e.g., Shanmugam, 2008a; Mutti et al., 2009; Stow et al., 2011, 2013). As pointed out by Stow et al. (2011, 2013), greater knowledge is required to differentiate sandy contourites or reworked turbidites from turbidites and to better understand their flow processes and genesis.

Well-sorted and clean sands, which were recognized in the Taiwan Canyon (Fig. 1) and are seen in core photographs of Fig. 2, were previously interpreted as modern reworked turbidites by Gong et al. (2015), based on evidence: (1) the widespread occurrence of diagnostic benthic foraminifera species for the recognition of the contour currents resulting from North Pacific Deep Water (NPIW-CCs), (2) the clean, well-sorted, and fine-grained properties, (3) the presence of sandy lags with sharp upper contacts overlain by finer-grained facies, (4) a lack of gradational upper contacts and of age inversion, (5) two- to three-subdivision grain size distribution patterns on cumulative frequency plots, and (6) abundant bio-skeletons, shell fragments, and foraminifer. Certainly, the same bottom current-reworked deposits (i.e., reworked turbidites as documented by Gong et al. (2012, 2015) should have been equally active in the geological past on the northern South China Sea margin. Nevertheless, flow processes and genesis of reworked turbidites still remain ambiguous. The current work focuses on the use of conventional cores from the middle Miocene Zhujiang Formation of the Pearl River Mouth

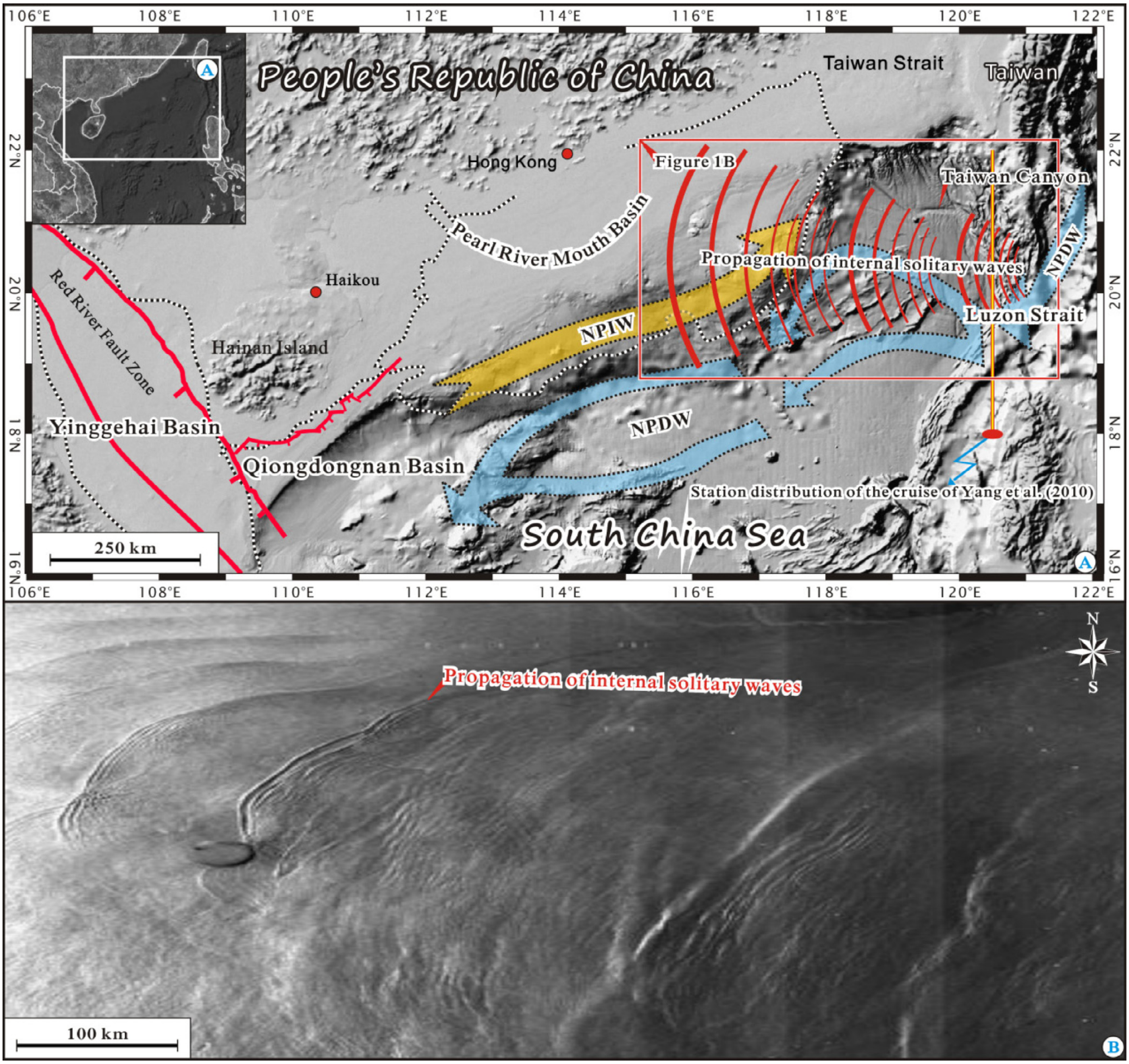

Fig. 1. (A) Bathymetry map showing the study area and main pathways of North Pacific Intermediate Water (NPIW) and North Pacific Deep Water (NPDW) (after Gong et al., 2013). Also shown are plan-view locations of Synthetic Aperture Radar image (image courtesy of C. Guo at the Ocean University of China) presented in (B). (B) The Synthetic Aperture Radar image showing the rapid propagation of internal solitary waves on the continental slope and adjacent abyssal plain of the northeastern South China Sea margin.

Please cite this article in press as: Gong, C., et al. Middle Miocene reworked turbidites in the Baiyun Sag of the Pearl River Mouth Basin, northern South China Sea margin: Processes, genesis, and implications. Journal of Asian Earth Sciences (2016), http://dx.doi.org/10.1016/j.jseaes.2016.06.025

Basin to: (1) investigate sedimentological characteristics of reworked turbidites and (2) address the flow processes, genesis, and implications of reworked turbidites, with an special attention of contour currents, internal waves and tides. Our work contributes to a better understanding of the flow processes and genesis of novel, non-turbidite reservoirs the potential economic interest.

2. Geological and oceanographic settings

The study area is located in the Pearl River Mouth Basin along the northern South China Sea margin (Fig. 1). The Pearl River Mouth Basin is a Cenozoic sedimentary basin, and underwent three main tectonic stages, namely Paleocene to early Oligocene rifting stage, late Oligocene transition stage, and early Miocene to Quaternary postrifting stage (Zhu et al., 2010; Franke et al., 2011; Franke, 2013; Zhao et al., 2016). Accordingly, the basin infill of the Pearl River Mouth Basin can be divided into three main supersequences, namely a syn-rift supersequence from Paleocene to early Oligocene, a transition supersequence of late Oligocene, and a post-rift supersequence from early Miocene to Quaternary (e.g., Gong et al., 2013; Zhao et al., 2016). Neritic, deltaic, and nearshore deposits were well developed within syn-rift and transition supersequences, whereas deep-water sedimentary systems became widely developed within post-rift supersequences in response to a prominent shelf-slope-basin physiography (Zhu et al., 2010; Franke et al., 2011; Franke, 2013; Zhao et al., 2016). Sandy turbidites in the post-rift supersequences are the focus of the present case study.

The modern ocean circulation in the South China Sea shows a sandwich-like pattern consisting of the seasonal surface-water circulation, the intermediate water circulation resulting from the North Pacific Intermediate Water (NPIW), and the deep-water

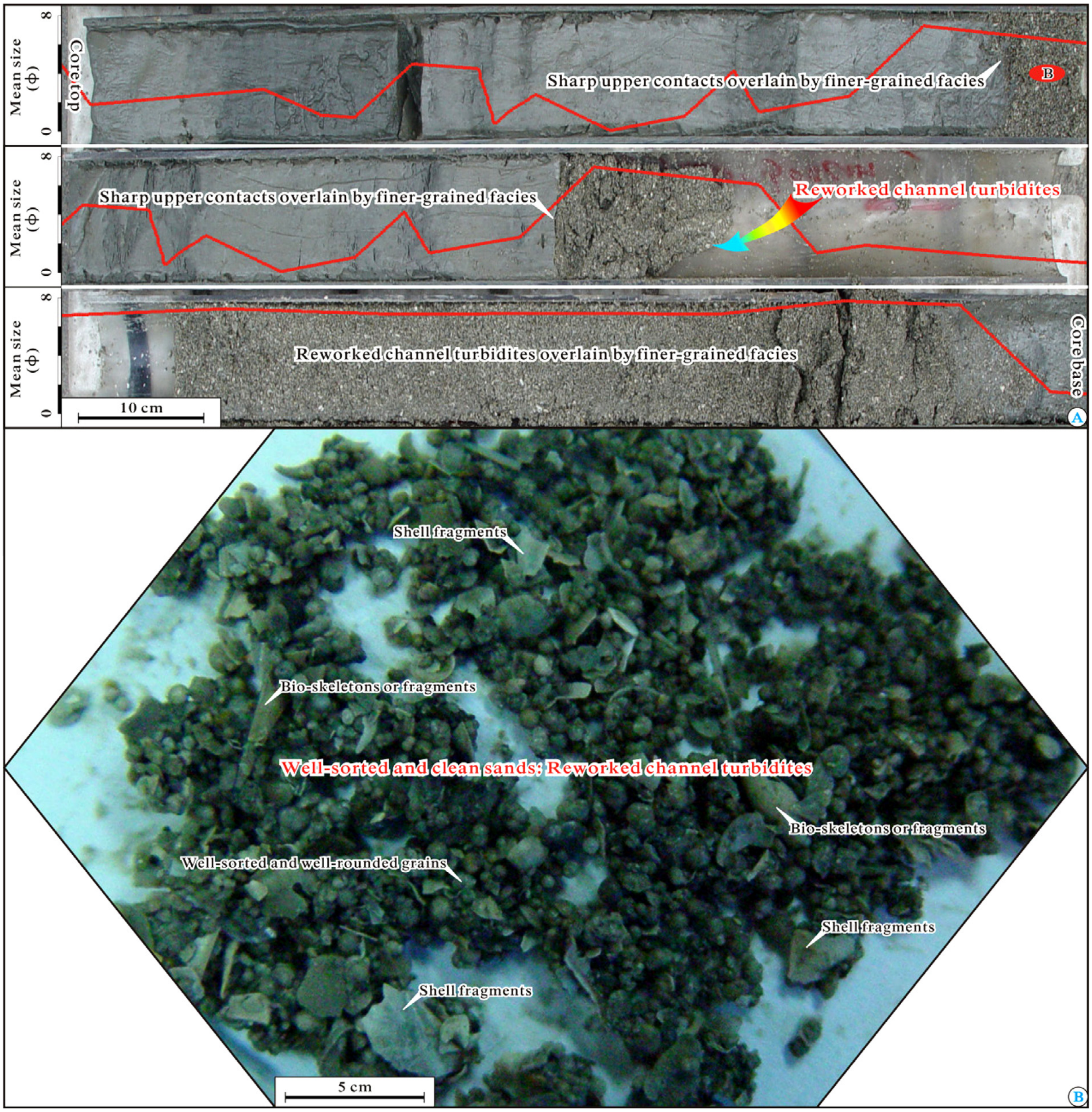

Fig. 2. Photographs of piston core (from Gong et al., 2015) taken from the Taiwan Canyon (Fig. 1) showing a close-up view of high net to gross ratio, clean, well-sorted sands that are interpreted as modern reworked turbidites in the Taiwan Canyon (see Gong et al., 2015 for further details).

Please cite this article in press as: Gong, C., et al. Middle Miocene reworked turbidites in the Baiyun Sag of the Pearl River Mouth Basin, northern South China Sea margin: Processes, genesis, and implications. Journal of Asian Earth Sciences (2016), http://dx.doi.org/10.1016/j.jseaes.2016.06.025

circulation resulting from the North Pacific Deep Water (NPDW) (Fig. 1) (Qu et al., 2006; Yang et al., 2010; Zhu et al., 2010; Gong et al., 2013; He et al., 2013). The intermediate water circulation is clockwise with the effective depth of 350–1350 m, whereas the deep-water circulation is counter-clockwise with the effective depth of >1350 m (Fig. 1) (e.g., Zhu et al., 2010; Gong et al., 2013; He et al., 2013).

Another oceanographic characteristic of the South China Sea is that it hosts the world's largest observed internal solitary waves created by the strong tide-topography interactions above the eastern ridge in the Luzon Strait (Reeder et al., 2011; Guo and Chen, 2014; Alford et al., 2015). These solitary waves can be readily seen in the Synthetic Aperture Radar mage presented in Fig. 1B. They propagate westwards across the northeastern South China Sea margin with amplitudes exceeding 100 m, and dissipate large amounts of energy and sediments by turbulent interaction with the sea floor, resulting in sand dunes on the upper slope of the northeastern South China Sea (Reeder et al., 2011; Alford et al., 2015). Contour currents resulting from the NPIW (NPIW-CCs), together with these internal solitary waves and internal tides, strongly influenced deep-water sedimentation in the South China Sea (Zhu et al., 2010; Reeder et al., 2011; Gong et al., 2012, 2013; Li et al., 2013).

3. Database and terminology

The present case study is based on core data acquired and provided by the China National Offshore Oil Corporation (CNOOC). Conventional cores shown in Figs. 3–10 were taken mainly from channels in the middle Miocene Zhujiang Formation in the Baiyun Sag of the Pearl River Mouth Basin (Fig. 1). They were carefully examined for sedimentary structures, grain-size variations, and vertical facies changes. Samples (n = 68) were selected from them for grain-size analysis (cf. Sime and Ferguson, 2003), and were conducted by CNOOC.

A proliferation of nomenclature is employed to describe sandy deposits created or substantially reworked by bottom (contour) currents, such as sandy contourites, bottom current-reworked sands, and reworked turbidites, contourite sands, etc. (e.g., Shanmugam, 2006, 2012; Rebesco et al., 2014; Mutti and Carminatti, 2012; Brackenridge et al., 2013; Stow et al., 2013). Sandy contourites or contourite sands are those sands transported and deposited by along-slope (thermohaline-driven) contour currents (e.g., Brackenridge et al., 2013; Stow et al., 2013). Bottom current-reworked sands as defined by Shanmugam (2003, 2008a, 2012) in contrast, refer to sandy deposits developed in a much broader array of depositional

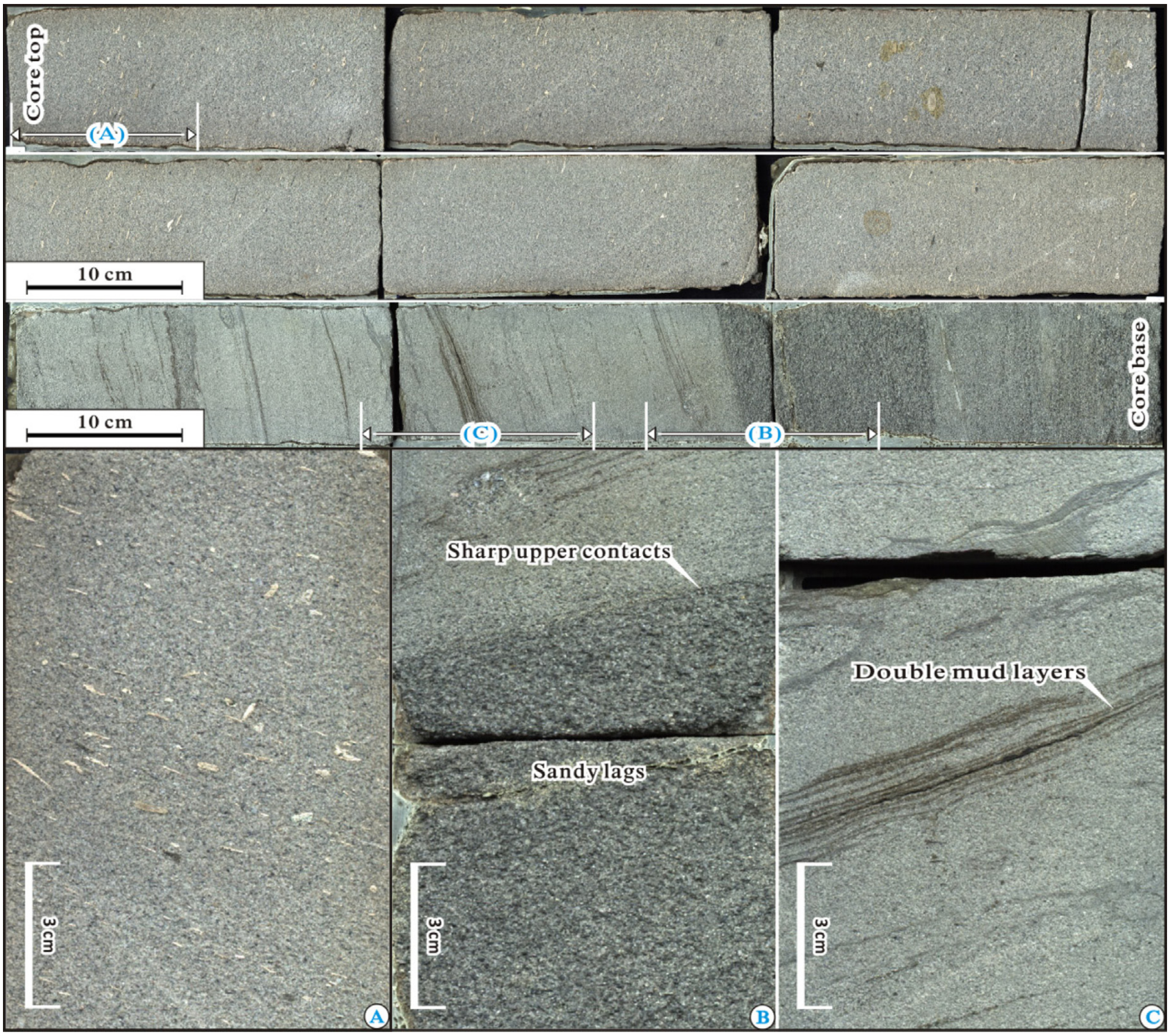

Fig. 3. (A) Core examples of ungraded sand facies composed of bioclastic-rich, fine- to medium-grained, clean, and well-sorted sands. (B) Core examples of sandy lags with sharp upper contacts overlain by finer-grained facies (white arrow). (C) Core photographs of clean well-sorted sands with double mud layers. Stratigraphic positions of core photographs presented in Figs. 3–9 are not shown because of the confidentially nature of them.

Please cite this article in press as: Gong, C., et al. Middle Miocene reworked turbidites in the Baiyun Sag of the Pearl River Mouth Basin, northern South China Sea margin: Processes, genesis, and implications. Journal of Asian Earth Sciences (2016), http://dx.doi.org/10.1016/j.jseaes.2016.06.025

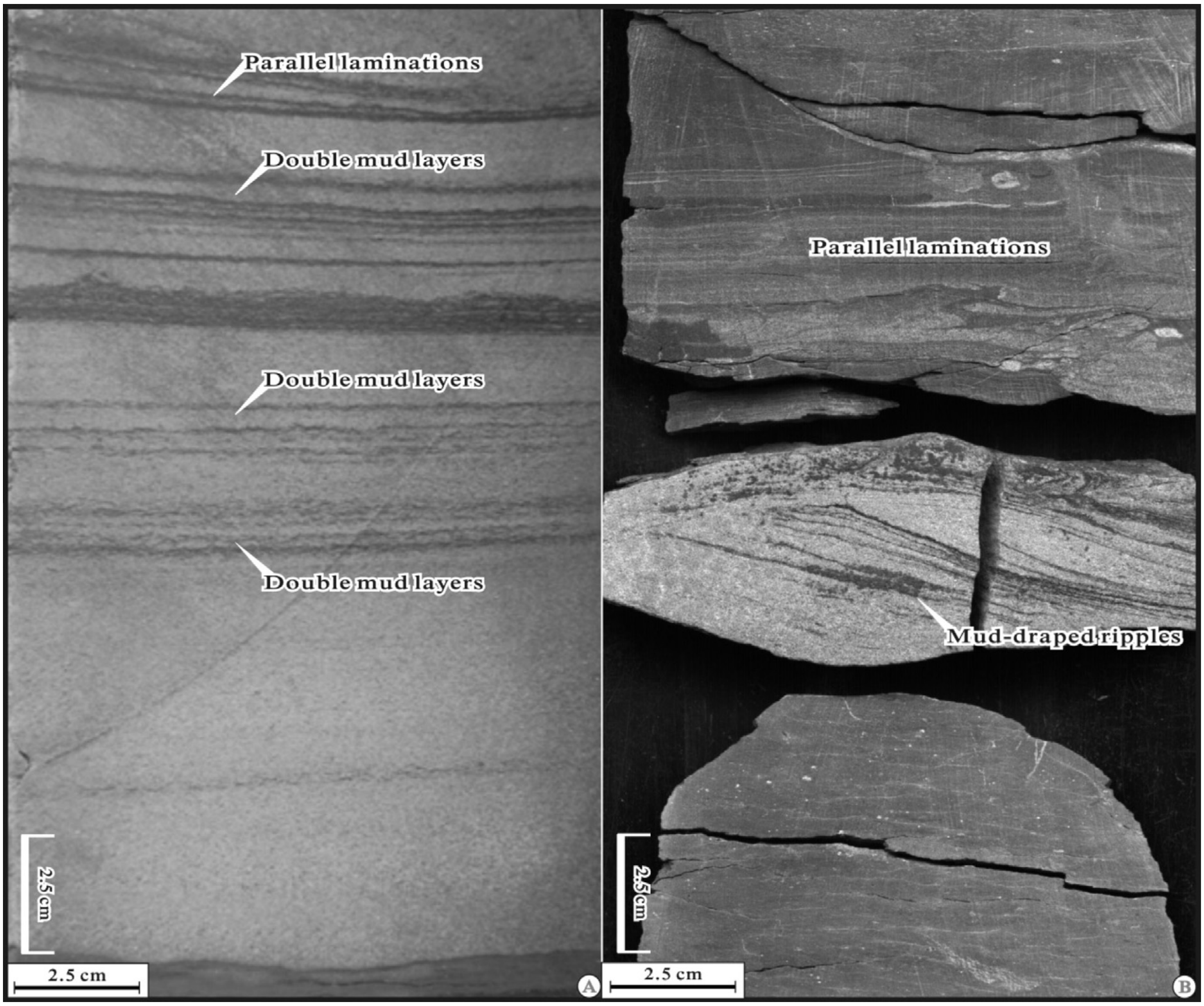

Fig. 4. (Panel A) Core photographs of ungraded sand facies showing well-developed parallel lamination and double mud layers. (Panel B) Core photographs illustrating discrete sand units with mud-offshoots.

environments (i.e., geostrophic bottom currents, wind driven bottom currents, and internal tides). Sandy deposits as documented in this case refer to remnants of turbidite beds showing evidence of strong action of bottom currents of a variety of origins, and tend to have a considerable down-slope sediment supply. As a result, the range of sedimentary structures seen in reworked turbidites are much more varied and not particularly described under the umbrella-term of sandy contourites. We therefore adopt the term 'reworked turbidites' (*sensu* Mutti and Carminatti, 2012) with a much broader meaning to define the interpreted sandy deposits.

4. Reworked turbidites recognized in conventional cores

4.1. Lithofacies description

Ungraded sand lithofacies were recognized in conventional cores taken from the middle Miocene Zhujiang Formation in the Baiyun Sag of the Pearl River Mouth basin (Figs. 3–10). Key sedimentological features of this lithofacies are listed as follows:

(1) They are composed of well-sorted, well rounded, and fine-grained sands or silts that are relatively free of mud (Figs. 3–9).
(2) They are rich in bio-skeletons that are aligned parallel or subparallel to the basal bedding and contain sandy lags with sharp upper contacts overlain by finer-grained facies (Fig. 3A and B).
(3) Well-developed double mud layers (also known as mud couplets) were recognized in core photographs of Figs. 3C, 4A, 5A and 8B. Thin (1–2 mm thick) mud layers (dark color in core photographs of Figs. 4B and 5A) occasionally drape sand ripples, forming so-called 'mud-draped ripples' (*sensu* Shanmugam, 2008b).
(4) Ripple laminations and low-angle cross laminations are found in the middle of core photographs of Fig. 5A. Thin (1–2 mm thick) sand layers, which are subparallel to each other (i.e., parallel lamination), were recognized in this core photographs of Figs. 5B and 7A.
(5) Well-developed flaser bedding (Figs. 6A, B and 8B), parallel lamination (Figs. 4A, B, 5B and 7B), bi-directional cross-laminations (Fig. 7B), wavy bedding (Fig. 8A), and lenticular bedding (Fig. 9B) have been recognised within the interpreted sandy facies.
(6) Ungraded lithofacies are intensely bioturbated and are rich in *Globigerina* (pelagic foraminifers) and in benthonic and planktonic foraminifers (Figs. 3A, 6A and 10), in which no gradational upper contacts were found (Figs. 3–10).

Please cite this article in press as: Gong, C., et al. Middle Miocene reworked turbidites in the Baiyun Sag of the Pearl River Mouth Basin, northern South China Sea margin: Processes, genesis, and implications. Journal of Asian Earth Sciences (2016), http://dx.doi.org/10.1016/j.jseaes.2016.06.025

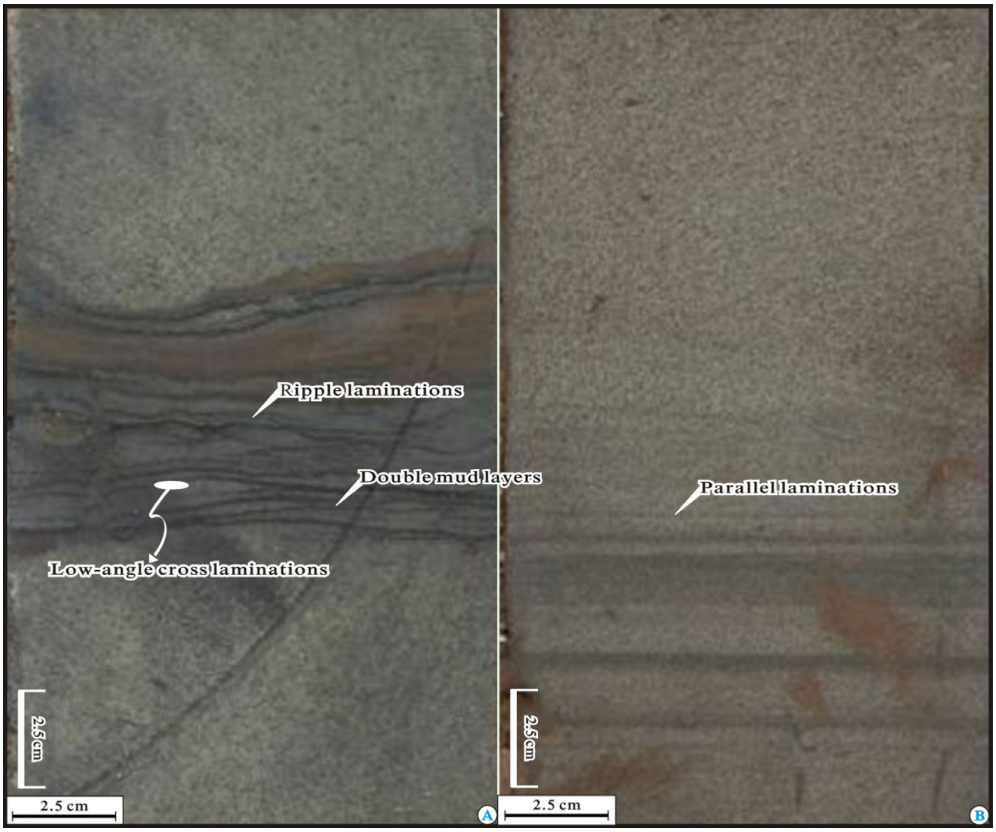

Fig. 5. (Panel A) Core examples of fine-grained sandstones displaying ripple lamination, mud-offshoots, double mud layers, and low-angle cross-lamination. (Panel B) Core examples of parallel laminations seen in ungraded sand facies.

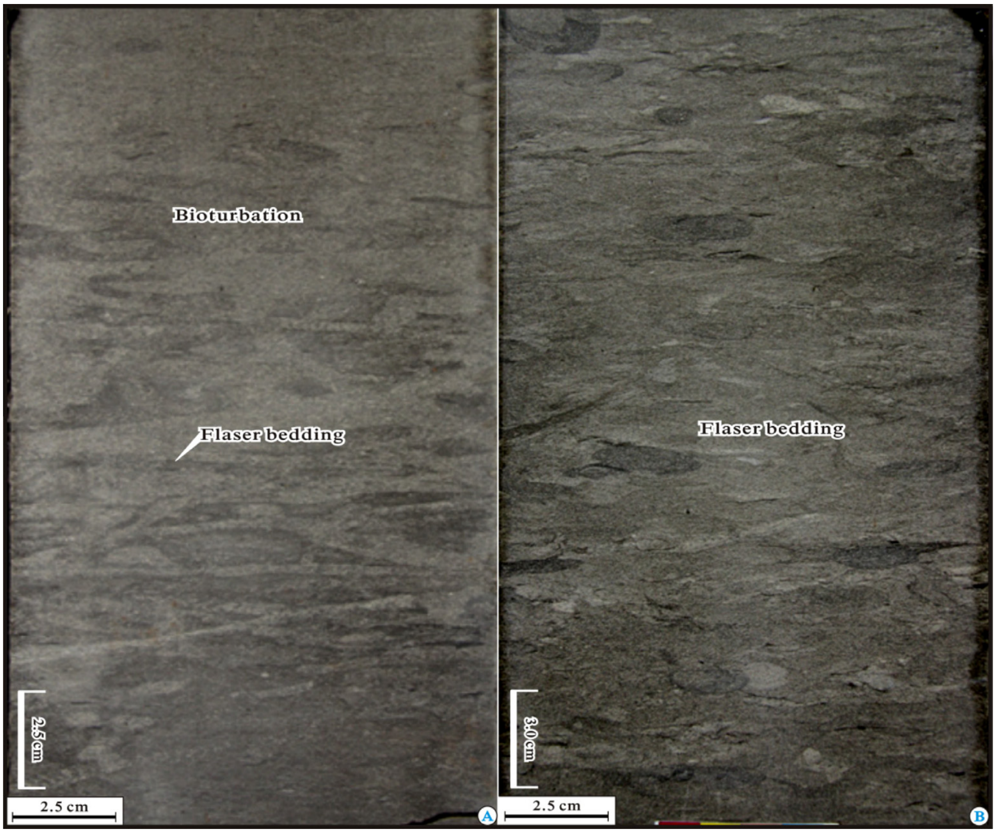

Fig. 6. Core examples of bioturbation and flaser bedding recognized in ungraded sand facies.

Please cite this article in press as: Gong, C., et al. Middle Miocene reworked turbidites in the Baiyun Sag of the Pearl River Mouth Basin, northern South China Sea margin: Processes, genesis, and implications. Journal of Asian Earth Sciences (2016), http://dx.doi.org/10.1016/j.jseaes.2016.06.025

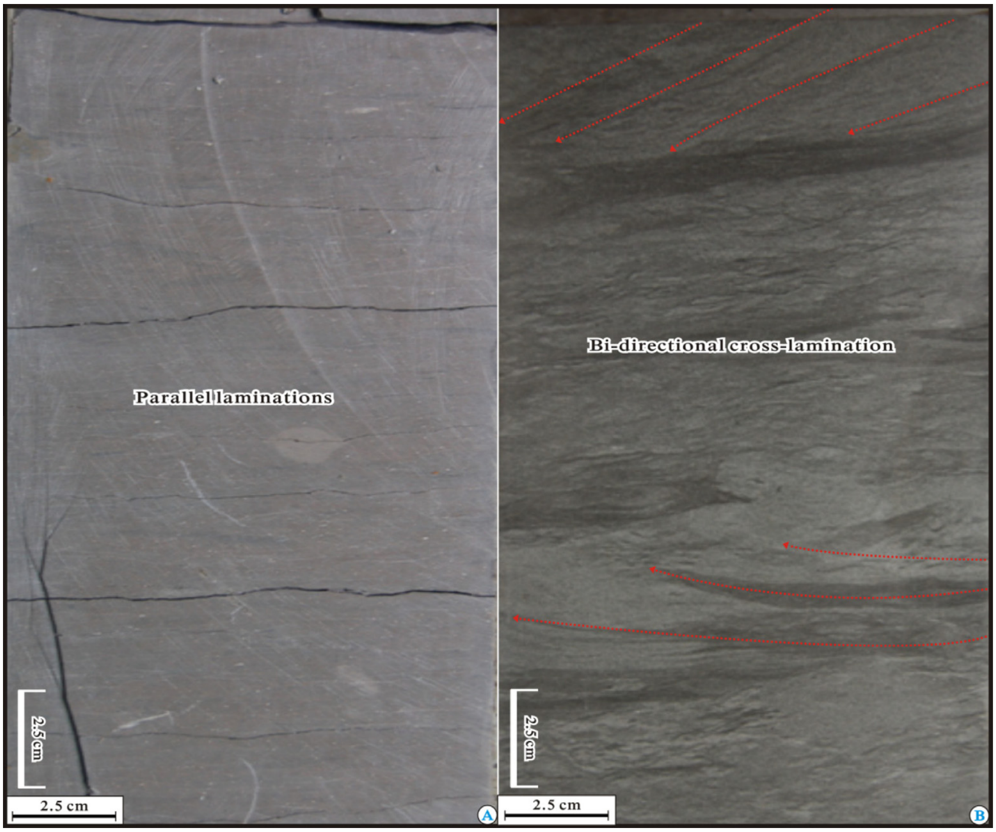

Fig. 7. Core examples of parallel laminations and bi-directional cross-lamination recognized in ungraded sand facies (left and right panels, respectively).

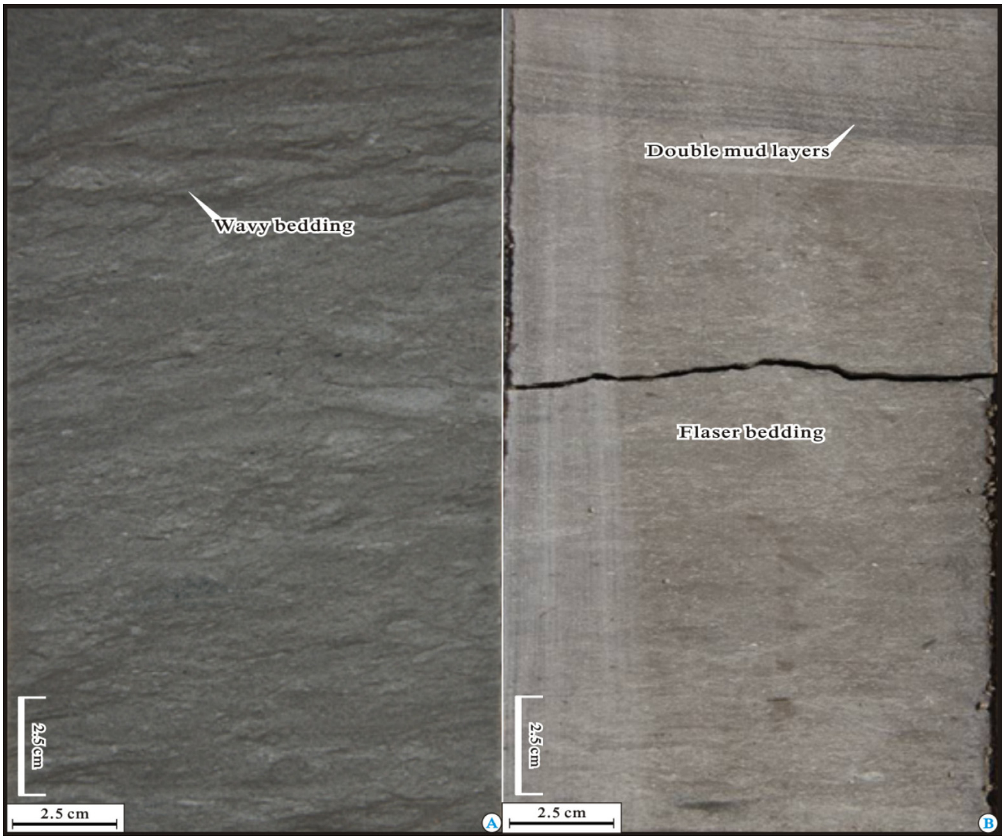

Fig. 8. Core examples of wavy bedding, flasher bedding, and double mud layers seen in ungraded sand facies that are interpreted as reworked channel turbidites.

Please cite this article in press as: Gong, C., et al. Middle Miocene reworked turbidites in the Baiyun Sag of the Pearl River Mouth Basin, northern South China Sea margin: Processes, genesis, and implications. Journal of Asian Earth Sciences (2016), http://dx.doi.org/10.1016/j.jseaes.2016.06.025

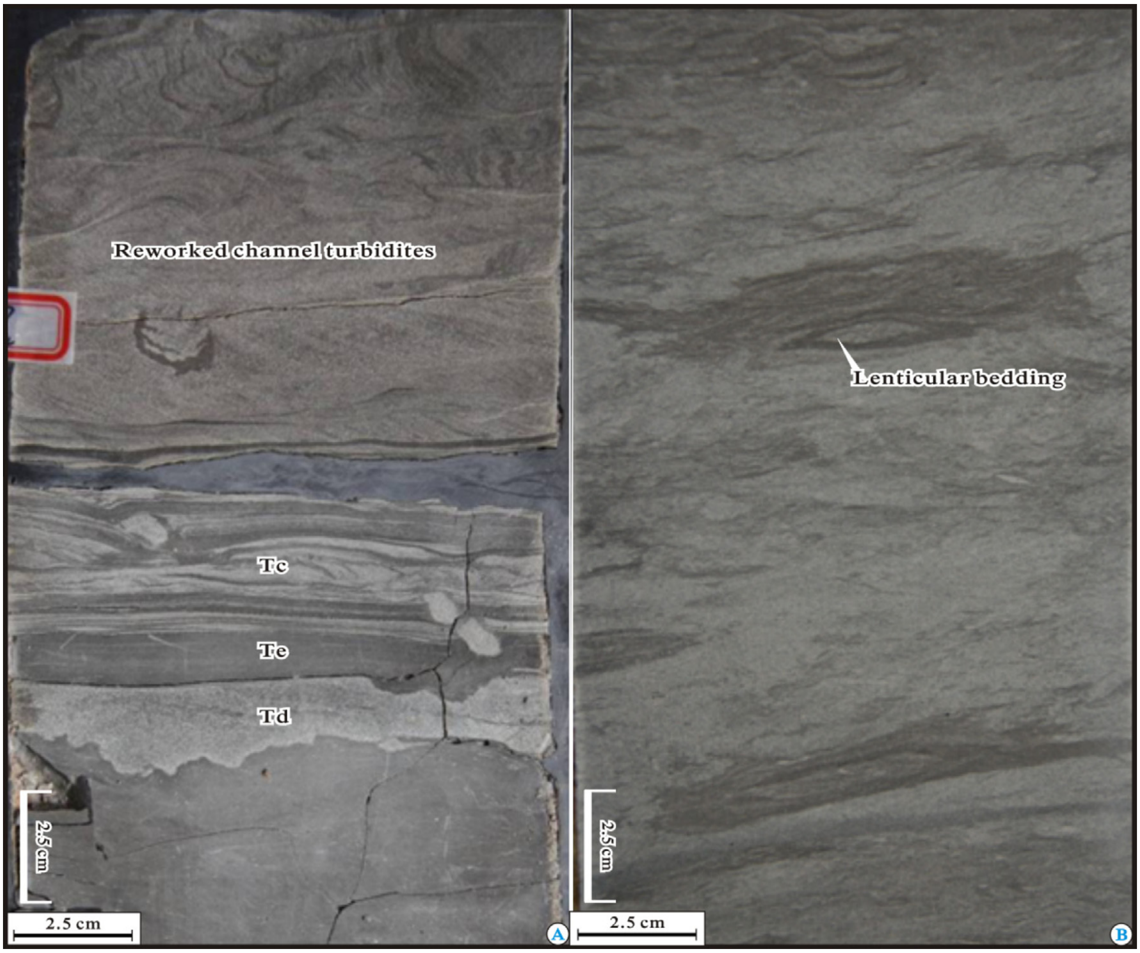

Fig. 9. Core photographs showing a blown-up view of reworked channel turbidites with lenticular bedding. Conventional cores shown in Figs. 3–9 were mainly taken from the middle Miocene Zhujiang Formation in the Baiyun Sag of the Pearl River Mouth Basin.

(7) They show a tripartite subdivision on cumulative frequency plots, consisting of a coarser-grained bedload fraction moved by traction, an intermediate fraction associated with saltation load, and a finer-grained fraction transported wholly in suspension (Fig. 11).

4.2. Lithofacies interpretation

The following seven lines of observations suggest that both turbidity flows and bottom currents were involved in the construction of ungraded sand lithofacies, forming reworked turbidites.

(1) High net to gross ratio and well sorted and fine-grained properties of the ungraded sand lithofacies suggest that winnowing and sorting processes, probably produced by bottom currents, were very effective during the deposition of them (Figs. 3–10) (see also Bouma and Hollister, 1973; Shanmugam, 2008a).

(2) Sandy lags with sharp upper contacts overlain by finer-grained deposits (Fig. 3B) and no gradational upper contacts were found in ungraded sand lithofacies (Figs. 3–10), indicating that both persistent action of bottom currents and episodic events of waning turbidity currents were collectively active. This interpretation is based on the assumption that sedimentary contacts would be erosional or gradational if only waning turbidity currents were active (cf., Shanmugam, 2008a; Gong et al., 2012, 2015). Clean, well sorted, and fine-grained sandy deposits have also been documented by Stow and Faugères (2008) and Shanmugam (2012) and were thought to be one of the possible modified sequence of sandy deposits affected by bottom currents.

(3) The mud-draped ripples indicating oscillating energy conditions were recognized in ungraded sand lithofacies (Figs. 4B and 5A), suggesting that bottom currents of tidal origin (i.e., internal tides) were probably involved in the construction of ungraded sand lithofacies. This interpretation is based on the belief that tidal bottom currents generally exhibit oscillating energy conditions, whereas turbidity flows generally show waning energy (e.g., Shanmugam, 2003, 2008a, 2012).

(4) Grain-size analyses indicate that ungraded sand lithofacies show characteristics of traction-current deposits, suggesting that they were reworked by deep-water traction currents (i.e., bottom currents) (Fig. 11) (e.g., Martin-Chivelet et al., 2008). Furthermore, tripartite subdivision grain size distribution patterns are also not a character of turbidites (Fig. 11), because turbidity currents generally transport fine-grained sand and mud wholly by suspension and the resultant turbidites generally show single segment grain size distribution patterns (e.g., Shanmugam, 2000). One of the most distinctive sedimentary features and structures seen in these lithofacies is that they occur in discrete units rather than forming a vertical sequence of structures (Figs. 3–10), indicating that they do not fix with the interpretation of classic turbidites.

Please cite this article in press as: Gong, C., et al. Middle Miocene reworked turbidites in the Baiyun Sag of the Pearl River Mouth Basin, northern South China Sea margin: Processes, genesis, and implications. Journal of Asian Earth Sciences (2016), http://dx.doi.org/10.1016/j.jseaes.2016.06.025

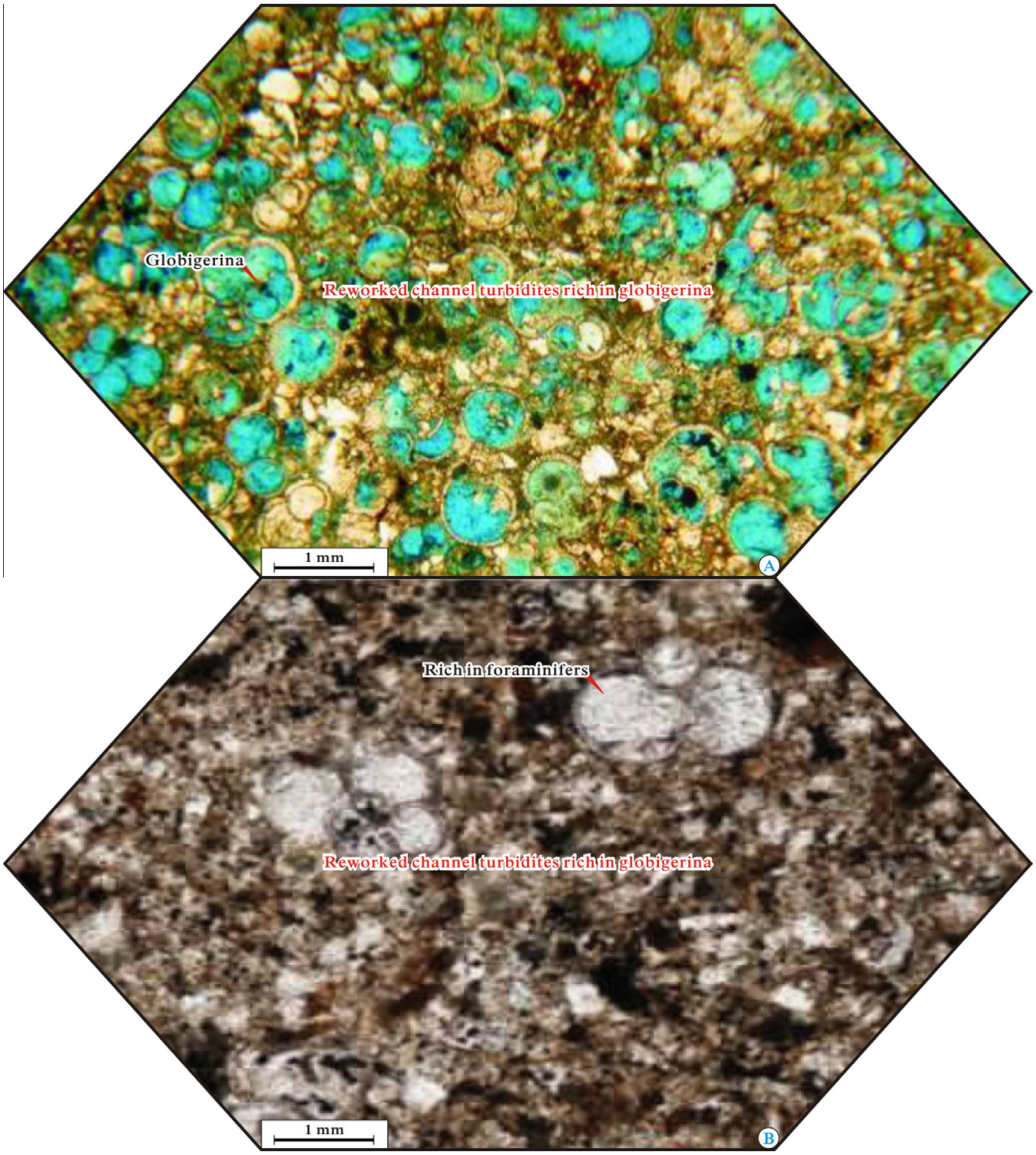

Fig. 10. (A) Scanning electron microscope images of core samples collected from ungraded sand facies that are rich in *Globigerina* (pelagic foraminifers). (B) Scanning electron microscope images of ungraded sand facies rich in benthonic and planktonic foraminifers.

(5) As shown in cores photographs of Fig. 12, coarse-grained debris-flow deposits are seen as the preservation of delicate mud fragments with planar fabric in coarse-grained sandy matrix. Compared with these coarse-grained debris-flow deposits, ungraded sand lithofacies are finer (Figs. 3–10), suggesting that ungraded sand lithofacies cannot be considered as sandy debris-flow deposits.

(6) The primary features seen in conventional cores (i.e., consisting of well-sorted, well rounded, and fine-grained sands or silts, rich in foraminifers and bio-skeletons, bioturbation, widespread occurrence of sandy lags with sharp upper contacts overlain by finer-grained facies, etc.) are broadly similar to observations seen in modern reworked turbidites occurring within the right-hand sides of the Taiwan Canyon (looking downstream) (Gong et al., 2015) (Fig. 2). But, the classic Bouma Sequence for turbidites (Bouma, 1962) cannot be used in interpreting and describing these deep-water deposits. In addition they are presenting traction structures, suspension features, and tidal signatures (Figs. 3–10). Therefore, these sandy lithofacies could be considered as reworked turbidites (*sensu* Mutti and Carminatti, 2012).

5. Flow processes of reworked turbidites as documented in this work

5.1. Along-slope contour currents

Unidirectionally migrating deep-water channels are reported to develop on the slope of the northern South China Sea margin (e.g., Zhu et al., 2010; Gong et al., 2013). This, coupled with the fact that contour currents are through to persist for a relatively long time (i.e., million-year scale), suggests that along-slope contour currents

Please cite this article in press as: Gong, C., et al. Middle Miocene reworked turbidites in the Baiyun Sag of the Pearl River Mouth Basin, northern South China Sea margin: Processes, genesis, and implications. Journal of Asian Earth Sciences (2016), http://dx.doi.org/10.1016/j.jseaes.2016.06.025

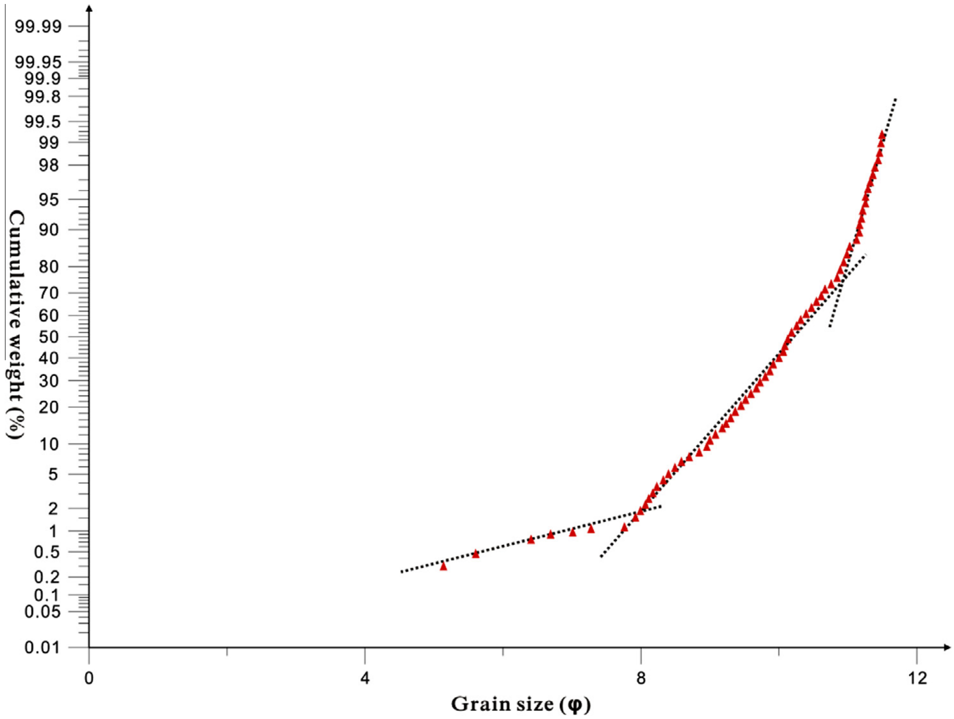

Fig. 11. Cumulative frequency plots of ungraded sand lithofacies seen in conventional cores. Curves presented in this figure were plotted based on 68 samples collected from conventional cores.

(i.e., NPIW-CCs) were probably involved in the construction of reworked turbidites recovered from deep-water sites. In addition, parallel-laminated silts as presented in Figs. 4A, B, 5B and 7A are broadly similar to contourite sandstones documented by Mutti and Carminatti (2012), Shanmugam (2008a) and Stow et al. (2008). This also suggests that along-slope contour currents of NPIW-CCs were probably involved in the formation of these documented reworked turbidites (Fig. 13).

5.2. Down-slope depositional processes

5.2.1. Turbidity currents

Reworked turbidites consist of fine- to medium-grained sands (mean size of 2–7 Φ) (Figs. 3–10), suggesting that long-axis-flowing turbidity currents were the dominant processes during the deposition of reworked turbidites (Fig. 13). This interpretation is based on the assumption that only turbidity currents could provide sufficient shear stress to erode underlying strata and transported coarse grains down-slope (e.g., Stigter et al., 2011; Mulder et al., 2012).

5.2.2. Internal waves and tides

Bidirectional cross-laminated, fine-grained internal-tide deposits were first recognized in the Middle Ordovician submarine channels in the southern Appalachians, USA by Gao and Eriksson (1991). He et al. (2011) interpreted ancient strata with bi-directional cross-lamination, wavy bedding and lenticular bedding as products of internal waves and internal tides. Pomar et al. (2012), Mazumder and Arima (2013) and Shanmugam (2013) have collectively suggested that the presence of tidal signatures (i.e., bi-directional cross-lamination, double mud layers, flaser bedding, wavy bedding, and lenticular bedding) in deep-water settings provides sedimentologic information for reading internal tides. Based on studies of the Deep Sea Drilling Project (Leg 30, sites 288 and 289), Klein (1975) interpreted clean well-sorted sands with mud-draped ripples and parallel lamination as the products of alternate traction and suspension deposition resulting from deep-water tidal bottom currents. Based on these observations, the interpreted reworked turbidites, which display double mud layers (Figs. 3C, 4A, 5A and 8B), flaser bedding (Figs. 6A, B and 8B), lenticular bedding (Fig. 9B), and bi-directional cross-lamination (Fig. 7B), can be best considered as products of internal waves and tides. Internal waves and tides, therefore, also have a profound influence on the development of the documented reworked turbidites (Fig. 13).

6. Genesis of reworked turbidites as studied in this work

6.1. Down-slope transport and reworking

Internal tides are able to attain velocities of 25–50 cm/s, and deep-water internal tides with maximum velocities up to 100 cm/s were measured from Gaoping deep-water channels on the southwestern Taiwan margin, by which even gravel grade grains can be transported and deposited (e.g., Shanmugam, 2003; Lee et al., 2009). Internal waves are commonly characterized by maximum vertical velocities of *ca* 20 cm/s, maximum horizontal velocities of *ca* 200 m/s, and by maximum speeds of >50 cm/s (e.g., Shanmugam, 2013). Internal waves in the northeastern South China Sea margin have maximum velocities of *ca* 30–40 cm/s and are able to cause movement of a wide range of sediment sizes, resulting in sand dunes on the upper slope of this margin (Fig. 2B) (Reeder et al., 2011; Guo and Chen, 2014; Alford et al., 2015). Clastic detritus fed to deep-water channels would be transported down-slope by turbidity flows, but could also be effectively resuspended, reworked and redeposited by up- and down-channel flowing internal tides and waves (Fig. 13). Such down-channel transport and reworking most likely yielded well-developed tidal signatures (i.e., double mud layers, flaser bedding, lenticular bedding, and biodirectional cross-bedding) (Figs. 3C, 4, 5A, 6, 7B, 8 and 9).

Please cite this article in press as: Gong, C., et al. Middle Miocene reworked turbidites in the Baiyun Sag of the Pearl River Mouth Basin, northern South China Sea margin: Processes, genesis, and implications. Journal of Asian Earth Sciences (2016), http://dx.doi.org/10.1016/j.jseaes.2016.06.025

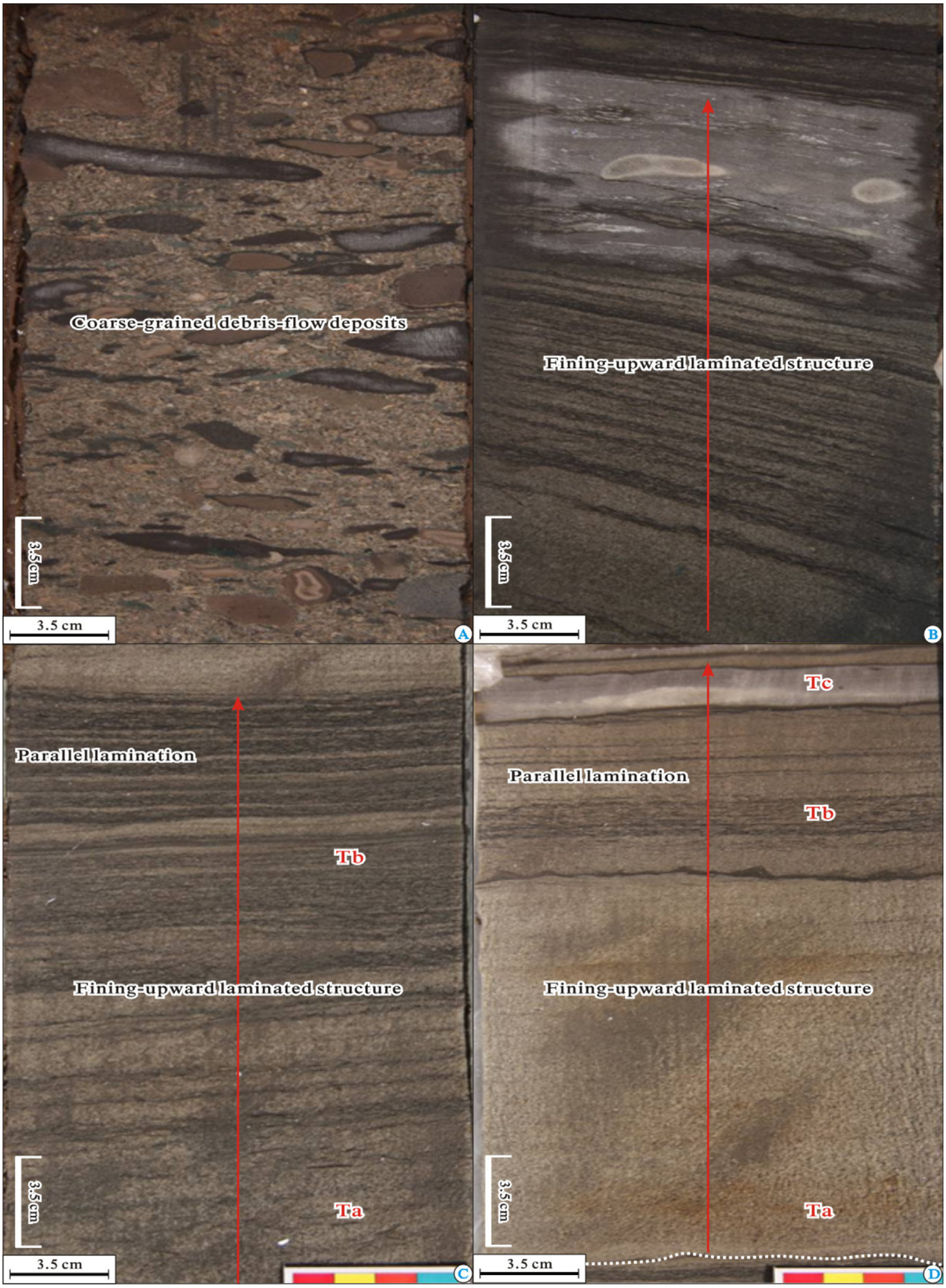

Fig. 12. Core photographs taking from the northern South China Sea margin illustrating architectural details of the coarse-grained debris-flow deposits. Note that structures seen in core photographs presented in this figure vertically organized into a fining-upward laminated Bouma Sequence rather than occurring in discrete units as seen in core photos of Figs. 3–9.

6.2. Along-slope winnowing and sorting

Yang et al. (2010) have suggested that along-slope contour currents of NPIW-CCs have a maximum velocity of 10 cm/s at the water depth of 700 m (see Fig. 1A for station distribution of the cruise of Yang et al., 2010). Previous studies suggest that contour currents flowing across narrow conduits (e.g., deep-water channels) will be accelerated, resulting in the accelerated contour currents that have flow velocities of 1–20 cm/s, with exceptionally strong contour currents with velocities up to of *ca* 50 cm/s

Please cite this article in press as: Gong, C., et al. Middle Miocene reworked turbidites in the Baiyun Sag of the Pearl River Mouth Basin, northern South China Sea margin: Processes, genesis, and implications. Journal of Asian Earth Sciences (2016), http://dx.doi.org/10.1016/j.jseaes.2016.06.025

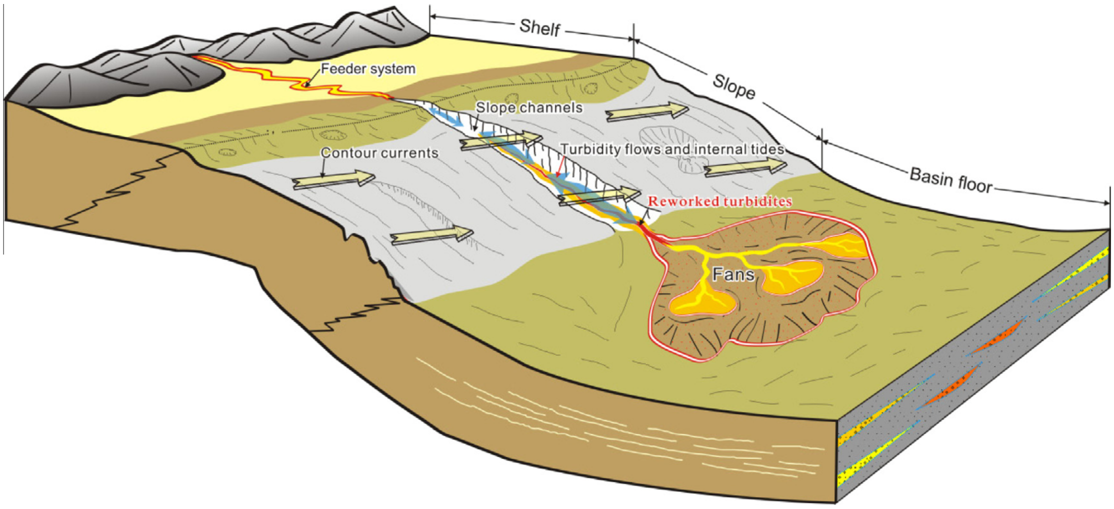

Fig. 13. Cartoon-style illustration of the flow processes and genesis of reworked turbidites. Note that reworked turbidites were created by the combined action of down-slope transport and reworking and along-slope winnowing and sorting.

(e.g., Stow et al., 2009; Shanmugam, 2008a, 2012). Therefore, contour currents of the accelerated NPIW-CCs may have maximum velocities of up to 10 cm/s, which are able to winnow away muddy fines. Regions of bottom water acceleration through narrow conduits contributed to extensive contourite sand accumulation (Gulf of Cadiz Sand Sheet) have been documented in the eastern Gulf of Cadiz by Hernández-Molina et al. (2006), Stow et al. (2011, 2013) and Brackenridge et al. (2013).

Energetic turbidity flows would have transformed into dilute, sluggish turbidity currents (cf. Jobe et al., 2011). Upper parts of these dilute turbidity currents would mix vertically with the seawater, supplying fine material to contour currents. These muddy fines carried within upper parts of dilute, sluggish turbidity currents would be effectively winnowed away by contour currents, whereas lower parts of these dilute turbidity currents will drop their coarse particles, forming remnants of turbidite beds exhibiting traction structures (i.e., tripartite subdivision grain size distribution patterns, CM values of sediment moved by traction, and unimodal grain-size distribution patterns) (Fig. 13).

7. Sedimentological and exploration significance

7.1. Approach to a better understanding of non-turbidite reservoirs

Our work has demonstrated that reworked turbidites show good hydrocarbon reservoir properties with high porosities and permeabilities (Figs. 2–10). Compared with their turbidite counterparts, the flow processes and genesis of reworked turbidites remain little documented (e.g., Mutti and Carminatti, 2012). We present here a model suggests which that reworked turbidites were created by combined action of down-slope transport and reworking and along-slope winnowing and sorting (Fig. 13). In the down-slope direction, clastic detritus were transported by turbidity flows, and would be bidirectionally reworked by internal waves and tides at the same time (Fig. 13), resulting in well-develop tidal signatures seen in reworked turbidites. In the along-slope direction, upper parts of dilute turbidity currents supplied muddy fines to contour currents, which were then winnowed away, allowing coarse particles carried within the lower parts of dilute turbidity currents to be eventually deposit as reworked turbidites lacking 'typical' turbidite signatures. This study contributes to a better understanding of the flow processes and genesis of deep-marine non-turbidite reservoirs.

7.2. Diagnostic criteria for the recognition of reworked turbidites

As pointed out by several authors (e.g., Viana, 2008; Hernández-Molina et al., 2011; Stow et al., 2011, 2013; Brackenridge et al., 2013), a robust set of diagnostic criteria for the recognition of non-turbidite sands (e.g., reworked turbidites) has yet to be developed. In terms of sedimentary facies, well-sorted and clean lithofacies recognized in piston cores (Fig. 2) and ungraded sand lithofacies seen in conventional cores (Figs. 3–10) are collectively interpreted as reworked turbidites. They exhibit the following features: (1) consisting of high net-to-gross ratio, clean, well-sorted and fine-grained sands (Figs. 2–10); (2) rich in bio-skeletons, shell fragments, foraminifers, pyrite, and quartz (Figs. 2, 3 and 8); (3) extensive bioturbation (Figs. 3, 7A and 10A); (4) displaying traction structures that occur in discrete units; and (5) exhibiting tidal signatures (i.e., double mud layers and mud-draped ripples, flaser bedding, wavy bedding, lenticular bedding, and bi-directional cross-lamination) (Figs. 3–10).

Although many features listed above can be attributed to either turbiditic origin or bottom-current reworking, the association of the several of them will enhance the chance of distinguishing reworked turbidites from other depositional facies. Sedimentological characteristics as noted herein, therefore, will help to obtain a robust set of diagnostic criteria for the recognition of novel, non-turbidite reservoir targets on continental margins worldwide. However, one must be aware that no single sedimentological characteristics as noted hereon are unique to reworked turbidites.

8. Conclusions

The present study focuses on the use of core data from the middle Miocene Zhujiang Formation in the Baiyun Sag of the Pearl River Mouth Basin to understand flow processes and genesis of reworked turbidites, and reveals that.

In terms of sedimentary facies, there are a robust set of diagnostic criteria for the recognition of reworked turbidites, but a distinctive attribute of them is their traction structures and tidal signatures that occur in discrete units rather than forming a classic Bouma Sequence. Sedimentological characteristics of reworked turbidites proposed here contribute to develop a robust set of diagnostic criteria for the recognition of reworked turbidites, and have practical implications for the recognition of non-turbidite reservoirs.

Please cite this article in press as: Gong, C., et al. Middle Miocene reworked turbidites in the Baiyun Sag of the Pearl River Mouth Basin, northern South China Sea margin: Processes, genesis, and implications. Journal of Asian Earth Sciences (2016), http://dx.doi.org/10.1016/j.jseaes.2016.06.025

In the down-slope direction, upper parts of dilute turbidity currents would mix vertically with sea water, and their associated muddy fines would be winnowed away by contour currents, whereas their lower parts would drop coarse particles within channels. In the along-slope direction, upper parts of dilute turbidity currents would mix vertically with seawater, and their associated muddy fines would be winnowed away by contour currents, whereas their lower parts would drop coarse particles, resulting in reworked turbidites displaying traction structures. Our work highlights the flow processes and genesis of reworked turbidites, helping to obtain a better understanding of the flow processes and genesis of non-turbidite reservoirs with a great economic interest.

Acknowledgments

Authors are grateful to CNOOC for providing subsurface data and for allowing publication of this paper. We thank Kevin T. Pickering for taking the time to plough through an earlier version of this manuscript. We acknowledge interesting discussions with Jiwei Tian at the Ocean University of China on contour currents and internal tides and waves acting in the South China Sea. Authors are indebted to journal Editor (Mei-Fu Zhou) and reviewer for their critical but constructive comments that significantly improved this work, and to Shunli Li at China University of Petroleum (Beijing) for helping us draw Fig. 13. This study was jointly supported by the National Natural Science Foundation of China (Nos. 41372115 and 41302085). RioMAR sponsor companies are greatly acknowledged for their discussion and generous support of C. Gong's postdoctoral research at the Jackson School of Geosciences of the University of Texas at Austin. Research was conducted in the framework of the ''Drifters'' Research Group of the Royal Holloway University of London (UK).

References

Alford, M.H., Peacock, T., MacKinnon, J.A., Nash, J.D., Buijsman, M.C., Centuroni, L.R., Chao, S.-Y., Chang, M.-H., Farmer, D.M., Fringer, O.B., Fu, K.-H., Gallacher, P.C., Graber, H.C., Helfrich, K.R., Jachec, S.M., Jackson, C.R., Klymak, J.M., Ko, D.S., Jan, S., Johnston, T.M.S., Legg, S., Lee, I.-H., Lien, R.-C., Mercier, M.J., Moum, J.N., Musgrave, R., Park, J.-H., Pickering, A.I., Pinkel, R., Rainville, L., Ramp, S.R., Rudnick, D.L., Sarkar, S., Scotti, A., Simmons, H.L., St Laurent, L.C., Venayagamoorthy, S.K., Wang, Y.-H., Wang, J., Yang, Y.J., Paluszkiewicz, T., Tang, T.-Y., 2015. The formation and fate of internal waves in the South China Sea. Nature 521, 65–69.

Bouma, A.H., 1962. Sedimentology of Some Flysch Deposits: A Graphic Approach to Facies Interpretation. Elsevier, Amsterdam, p. 168.

Bouma, A.H., Hollister, C.D., 1973. Deep ocean basin sedimentation. In: Middleton, G.V., Bouma, A.H. (Eds.), Turbidites and Deep-Water Sedimentation: SEPM Pacific Section Short Course. Tulsa, Oklahoma, pp. 79–118.

Brackenridge, R.E., Hernández-Molina, F.J., Stow, D.A.V., Llave, E., 2013. A pliocene mixed contourite-turbidite system offshore the Algarve Margin, Gulf of Cadiz: seismic response, margin evolution and reservoir implications. Mar. Pet. Geol. 46, 36–50.

Franke, D., Barckhausen, U., Baristeas, N., Engels, M., Ladage, S., Lutz, R., Montano, J., Pellejera, N., Ramos, E.G., Schnabel, M., 2011. The continent ocean transition at the southeastern margin of the South China Sea. Mar. Pet. Geol. 28, 1187–1204.

Franke, D., 2013. Rifting, lithosphere breakup and volcanism: comparison of magma-poor and volcanic rifted margins. Mar. Pet. Geol. 43, 63–87.

Gao, Z., Eriksson, K.A., 1991. Internal-tide deposits in an Ordovician submarine channel: previously unrecognized facies. Geology 19, 734–737.

Gong, C., Wang, Y., Peng, X., Li, W., Qiu, Y., Xu, S., 2012. Sediment waves on the South China Sea Slope off southwestern Taiwan: implications for the intrusion of the North Pacific Deep Water into the South China Sea. Mar. Pet. Geol. 32, 95–109.

Gong, C., Wang, Y., Zhu, W., Li, W., Xu, Q., 2013. Upper Miocene to Quaternary unidirectionally migrating deed-water channels in the Pearl River Mouth Basin, northern South China Sea. AAPG Bull. 97, 285–308.

Gong, C., Wang, Y., Xu, S., Pickering, K.T., Peng, X., Li, W., Yan, Q., 2015. The northeastern South China Sea margin created by the combined action of down-slope and along-slope processes: processes, products and implications for exploration and paleoceanography. Mar. Pet. Geol. 64, 233–249.

Guo, C., Chen, X., 2014. A review of internal solitary wave dynamics in the northern South China Sea. Prog. Oceanogr. 121, 7–23.

He, Y., Xie, X., Kneller, B.C., Wang, Z., Li, X., 2013. Architecture and controlling factors of canyon fills on the shelf margin in the Qiongdongnan Basin, northern South China Sea. Mar. Pet. Geol. 41, 264–276.

He, Y., Luo, J., Li, X., Gao, Z., Wen, Z., 2011. Evidence of internal-wave and internal-tide deposits in the Middle Ordovician Xujiajuan formation of the Xiangshan Group, Ningxia, China. Geo-Mar. Lett. 31, 509–523.

Hernández-Molina, F.J., Llave, E., Stow, D.A.V., Garciad, M., Somoza, L., Vazqueze, J.T., Lobo, F.J., Maestro, A., del Ríog, V.D., León, R., Medlalaeab, T., Gardner, J., 2006. The contourite depositional system of the Gulf of Cadiz: a sedimentary model related to the bottom current activity of the Mediterranean outflow water and its interaction with the continental margin. Deep-Sea Res. II 53, 1420–1463.

Hernández-Molina, F.J., Stow, D.A.W., Liave, E., Rebesco, M., Ercilla, Van Rooij, G., Mena, A., Vazquez, J.T., Voelker, A.H.L., 2011. Deep-water circulation: processes & products (16–18 June 2010, Baiona): introduction and future challenges. Geo-Mar. Lett. 31, 285–300.

Hernández-Molina, F.J., Llave, E., Preu, B., Ercilla, G., Fontan, A., Bruno, M., Serra, N., Gomiz, J.J., Brackenridge, R.E., Sierro, F.J., Stow, D.A.V., García, M., Juan, C., Sandoval, N., Arnaiz, A., 2014. Contourite processes associated to the Mediterranean Outflow Water after its exit from the Gibraltar Strait: global and conceptual implications. Geology 42, 227–230.

Jobe, Z.R., Lowe, D.R., Uchytil, S.J., 2011. Two fundamentally different types of submarine canyons along the continental margin of Equatorial Guinea. Mar. Pet. Geol. 28, 843–860.

Klein, G. dev., 1975. Resedimented pelagic carbonate and volcaniclastic sediments and sedimentary structures in Leg 30 DSDP cores from the western equatorial Pacific. Geology 3, 39–42.

Lee, I.-H., Lien, R.-C., Liu, J.T., Chuang, W.-S., 2009. Turbulent mixing and internal tides in Gaoping (Kaoping) Submarine Canyon, Taiwan. J. Mar. Syst. 76, 383–396.

Li, Y., Zhen, R., Guo, G., Hu, X., 2012. Geological significance of deep-water traction deposits in Baiyun Sag, Pearl River Mouth Basin (in Chinese with English abstract). Acta Oceanographica Sin. 76, 127–135.

Li, H., Wang, Y., Zhu, W., Xu, Q., He, Y., Tang, W., Zhuo, H., Wang, D., Wu, J., Li, D., 2013. Seismic characteristics and processes of the Plio-Quaternary unidirectionally migrating channels and contourites in the northern slope of the South China Sea. Mar. Pet. Geol. 43, 370–380.

Martin-Chivelet, J., Fregenal-Martínez, M.A., Chacón, B., 2008. Traction structures in contourites. In: Rebesco, M., Camerlenghi, A. (Eds.), Contourites: Developments in Sedimentology, vol. 60. Elsevier Science, Amsterdam, pp. 159–182.

Mulder, T., Zaragosl, S., Garlan, T., Mavel, J., Cremer, M., Sottolichio, A., SeNechal, N., Schmidt, S., 2012. Present deep-submarine canyons activity in the Bay of Biscay (NE Atlantic). Mar. Geol. 295–298, 113–127.

Mutti, E., Bernoulli, D., Lucchi, F.R., Tinterri, R., 2009. Turbidites and turbidity currents from Alpine 'flysch' to the exploration of continental margins. Sedimentology 56, 267–318.

Mutti, E., Carminatti, M., 2012. Deep-Water Sands in the Brazilian Offshore Basins: AAPG Search and Discovery Article 30219 <http://www.searchanddiscovery.com/documents/2012/30219mutti/ndx_mutti.pdf>.

Nelson, C.H., Baraza, J., Maldonaldo, A., 1993. Mediterranean undercurrent sandy contourites, Gulf of Cadiz, Spain. Sed. Geol. 82, 103–131.

Nelson, C.H., Baraza, J., Maldonado, A., Rodero, J., Escutia, C., Barber, J.H., 1999. Influence of the Atlantic inflow and Mediterranean outflow currents on Late Quaternary sedimentary facies of the Gulf of Cadiz continental margin. Mar. Geol. 155, 99–129.

Palermo, D., Galbiati, M., Famiglietti, M., Marchesini, M., Mezzapesa, D., Fonnesu, F., 2014. Insights into a New Super-Giant Gas Field – Sedimentology and Reservoir Modeling of the Coral Complex, Offshore Northern Mozambique OTC-24907-MS.

Pomar, L., Morsilli, M., Hallock, P., Bádenas, B., 2012. Internal waves, an under-explored source of turbulence events in the sedimentary record. Earth Sci. Rev. 111, 56–81.

Qu, T., Girton, J.B., Whitehead, J.A., 2006. Deepwater overflow through Luzon Strait. J. Geophys. Res. 111, C01002. http://dx.doi.org/10.1029/2005JC003139.

Rebesco, M., Hernández-Molina, F.J., Van Rooij, D., Wåhlin, A., 2014. Contourites and associated sediments controlled by deep-water circulation processes: state of the art and future considerations. Mar. Geol. 352, 111–154.

Reeder, D.B., Barry, B.M., Yang, Y.J., 2011. Very large subaqueous sand dunes on the upper continental slope in the South China Sea generated by episodic, shoaling deep-water internal solitary waves. Mar. Geol. 279, 12–18.

Shanmugam, G., Spalding, T.D., Rofheart, D.H., 1993. Traction structures in deep-marine, bottom current-reworked sands in the Pliocene and Pleistocene, Gulf of Mexico. Geology 21, 929–932.

Shanmugam, G., 2000. 50 years of the turbidite paradigm (1950s–1990s): deep-water processes and facies models—a critical perspective. Mar. Pet. Geol. 17, 285–342.

Shanmugam, G., 2003. Deep-marine tidal bottom currents and their reworked sands in modern and ancient submarine canyons. Mar. Pet. Geol. 20, 471–491.

Shanmugam, G., 2006. Deep-Water Processes and Facies Models: Implications for Sandstone Petroleum Reservoirs: 5 (Handbook of Petroleum Exploration and Production). Elsevier Science, p. 496.

Shanmugam, G., 2008a. Deep-water bottom currents and their deposits. In: Rebesco, M., Camerlenghi, A. (Eds.), Contourites: Developments in Sedimentology, vol. 60. Elsevier Science, Amsterdam, pp. 59–83.

Shanmugam, G., 2008b. Leaves in turbidite sands: the main source of oil and gas in the deep-water Kutei Basin, Indonesia: Discussion. AAPG Bull. 92, 127–137.

Shanmugam, G., 2012. New Perspectives on Deep-Water Sandstones. Elsevier Science, Amsterdam, pp. 1–219.

Shanmugam, G., 2013. Modern internal waves and internal tides along oceanic pycnoclines: challenges and implications for ancient deep-marine baroclinic sands. AAPG Bull. 97, 799–843.

Sime, L.C., Ferguson, R.I., 2003. Information on grain sizes in gravel-bed rivers by automated image analysis. J. Sed. Res. 73, 630–636.

Stigter, C.H., Jesus, C.C., Boerr, W., Richter, T.O., Costa, A., van Weering, T.C.E., 2011. Recent sediment transport and deposition in the Lisbon-Setúbal and Cascais submarine canyons, Portuguese continental margin. Deep-Sea Res. II 58, 2321–2344.

Stow, D.A.W., Faugères, J.-C., 2008. Contourite facies and the facies model. In: Rebesco, M., Camerlenghi, A. (Eds.), Contourites: Developments in Sedimentology, vol. 60. Elsevier Science, Amsterdam, pp. 223–257.

Stow, D.A.W., Hunter, S., Wilkinson, D., Hernández-Molina, F.J., 2008. The nature of contourite deposition. In: Rebesco, M., Camerlenghi, A. (Eds.), Contourites: Developments in Sedimentology, vol. 60. Elsevier Science, Amsterdam, pp. 142–199.

Stow, D.A.V., Hernández-Molina, F.J., Llave, E., Sayago, M., Díaz del Río, V., Branson, A., 2009. Bedform-velocity matrix: the estimation of bottom current velocity from bedform observations. Geology 37, 327–330.

Stow, D.A.V., Brackenridge, R.E., Hernández-Molina, F.J., 2011. Contourite Sheet Sands: New Deepwater Exploration Target: AAPG Search and Discovery Article 30182 <http://www.searchanddiscovery.com/documents/2011/30182stow/ndx_stow.pdf>.

Stow, D.A.W., Hernández-Molina, F.J., Lave, E., Bruno, M., García, M., Díaz del RIO, V., Somoza, L., Brackenridge, R.E., 2013. The Cadiz Contourite Channel: Sandy contourites, bedforms and dynamic current interaction. Mar. Geol. 343, 99–114.

Viana, A.R., 2008. Economic relevance of contourites. In: Rebesco, M., Camerlenghi, A. (Eds.), Contourites: Developments in Sedimentology, vol. 60. Elsevier Science, Amsterdam, pp. 493–510.

Yang, Q., Tian, J., Zhao, W., 2010. Observation of Luzon Strait transport in summer 2007. Deep-Sea Res. I 57, 670–676.

Zhao, F., Alves, T.M., Wu, S., Li, W., Huuse, M., Mi, L., Sun, Q., Ma, B., 2016. Prolonged post-rift magmatism on highly extended crust of divergent continental margins (Baiyun Sag, South China Sea). Earth Planet. Sci. Lett. 445, 79–91.

Zhu, M., Graham, S., Pang, X., McHargue, T., 2010. Characteristics of migrating submarine canyons from the middle Miocene to present: implications for paleoceanographic circulation, Northern South China Sea. Mar. Pet. Geol. 27, 307–319.

Please cite this article in press as: Gong, C., et al. Middle Miocene reworked turbidites in the Baiyun Sag of the Pearl River Mouth Basin, northern South China Sea margin: Processes, genesis, and implications. Journal of Asian Earth Sciences (2016), http://dx.doi.org/10.1016/j.jseaes.2016.06.025